

Forkhead box protein C1 promotes cell proliferation and invasion in human cervical cancer

LU WANG, LULU CHAI, QINGCHUN JI, RONGJIE CHENG, JIAO WANG and SHIYU HAN

Department of Gynecology and Obstetrics, The Fourth Affiliated Hospital of Harbin Medical University, Harbin, Heilongjiang 150037, P.R. China

Received November 13, 2016; Accepted August 17, 2017

DOI: 10.3892/mmr.2018.8423

Abstract. Increasing evidence has demonstrated that aberrant forkhead box protein C1 (FOXC1) expression contributes to tumorigenesis in multiple types of malignant tumor. However, the clinical significance and biological roles of FOXC1 in cervical cancer remain unknown. The expression levels of FOXC1 were examined in human cervical cancer tissues and cells using reverse transcription-quantitative polymerase chain reaction, immunohistochemistry and western blotting. Furthermore, high FOXC1 expression was significantly associated with advanced clinical stages, a high degree of malignancy and a poor outcome. FOXC1 silencing inhibited cell growth and enhanced cell apoptosis. Knockdown of FOXC1 markedly suppressed cell migration and invasion *in vitro*, and resulted in downregulation of phosphorylated-RAC- α serine/threonine-protein kinase, proto-oncogene c-Myc and B-cell lymphoma 2. In conclusion, these data indicated that upregulation of FOXC1 contributed to the development of cervical cancer by increasing the growth and motility of the cervical cancer cells, thereby worsening the disease progression in these patients.

Introduction

Cervical cancer is the most common malignancy of the female genital tract and the second leading cause of mortality among women worldwide, with an estimated global incidence of >500,000 newly diagnosed cases and 260,000 mortalities annually (1,2). Persistent infection with high-risk human papillomavirus has been considered to be the primary risk factor for developing cervical cancer and its precursor lesions (3-6).

Although surgical resection combined with radiotherapy and chemotherapy has been used as a major treatment for patients with cervical cancer, the overall survival (OS) rate and disease-free survival rate for patients with late-stage disease remain poor (1,5,7). Therefore, understanding the molecular mechanisms underlying cervical cancer and identifying factors involved in the progression of the disease is important, in order to offer novel therapeutic targets and improve patient survival.

Forkhead box protein C1 (FOXC1), a member of the FOX family of transcription factors, is located on chromosome 6p25 and regulates an array of biological processes, including metabolism, development, differentiation, proliferation, apoptosis and cell migration (8-11). In addition to its roles in normal function and development, FOXC1 has been demonstrated to be a possible master regulator in various types of human cancer, including breast cancer, hepatocellular carcinoma, pancreatic and non-small cell lung cancers (8,9,11-13). In addition, high FOXC1 expression is correlated with poor clinical outcome (9,13-15). However, to the best of the authors' knowledge, expression of FOXC1 has not been investigated in cervical cancer. The aim of the present study was to investigate alterations in the expression of FOXC1 and the biological function of FOXC1 in cervical cancer cells *in vitro*.

Materials and methods

Patients and tissue specimens. Samples from patients aged 48-73 years (n=76) with cervical cancer who underwent curative surgical resection were collected from The Fourth Affiliated Hospital of Harbin Medical University (Harbin, China) between March 2009 and June 2011. A total of 34 control samples were obtained from women who underwent hysterectomy for nonmalignant conditions during the same period. None of the patients were treated with any preoperative therapy. The clinical and clinicopathological parameters, and staging, were defined according to the 2009 International Federation of Gynecology and Obstetrics (FIGO) criteria (16). The OS was defined as the time between surgery and mortality or the last follow-up examination, and the follow-up periods ranged between 19 and 84 months. Informed consent was obtained from all enrolled individuals and the present study was approved by the Ethics Committee of The Fourth Affiliated Hospital of Harbin Medical University. All tissue specimens were immediately snap-frozen in liquid nitrogen and stored at -80°C until RNA extraction.

Correspondence to: Dr Shiyu Han, Department of Gynecology and Obstetrics, The Fourth Affiliated Hospital of Harbin Medical University, 37 Yiyuan Street, Nangang, Harbin, Heilongjiang 150037, P.R. China
E-mail: shiyu962@163.com

Key words: forkhead box protein C1, cervical cancer, proliferation, migration

Cell lines. A total of four human cervical cancer cell lines (CaSki, HeLa, ME-180 and SiHa) (17) and the human immortalized cervical epithelial cell line (NC104) were purchased from the Type Culture Collection of the Chinese Academy of Sciences (Shanghai, China). All cell lines were cultured in Dulbecco's modified Eagle's medium (Hyclone; GE Health Care Life Sciences, Logan, UT, USA) supplemented with 10% fetal bovine serum (FBS; Gibco; Thermo Fisher Scientific, Inc., Waltham, MA, USA), 100 U/ml penicillin and 100 μ g/ml streptomycin at 37°C in a humidified incubator containing 5% CO₂.

Total RNA extraction and reverse transcription-quantitative polymerase chain reaction (RT-qPCR). Total RNA from cells and fresh tissue samples was extracted using TRIzol® (Invitrogen; Thermo Fisher Scientific, Inc.), according to the manufacturer's protocol. A total of 500 ng RNA was reversed transcribed into cDNA using the ReverTra Ace- α kit (Toyobo Life Science, Osaka, Japan), according to the manufacturer's protocol. qPCR was performed using SYBR® Premix Ex Taq™ II (Takara Biotechnology Co., Ltd., Dalian, China) with the ABI 7900 Fast Real Time PCR System (Applied Biosystems; Thermo Fisher Scientific, Inc.). The following thermocycling conditions were used: 95°C for 30 sec; followed by 40 cycles of 95°C for 5 sec and 60°C for 30 sec. Primers were designed and synthesized by Sangon Biotech Co., Ltd. (Shanghai, China). The following primers were used: FOXC1 sense, 5'-CTGCCCGACTACTCTCTGC-3' antisense, 5'-CACCGAGTGGAAAGTTCTGC-3'; and GAPDH sense, 5'-CGA GATCCCTCCAAAATCAA-3' and antisense, 5'-TTCACA CCCATGACGAACAT-3'. The fold-change in FOXC1 mRNA expression was calculated using the 2^{- $\Delta\Delta$ C_q} method following normalization to GAPDH expression (18).

Immunohistochemical (IHC) staining. IHC staining was performed as previously described (19). Collected tissue specimens were paraffin-embedded (Gene Company Ltd., Hong Kong, China) and cut into 4- μ m-thick sections. Following deparaffinization with xylene, the sections were submerged into citrate antigenic retrieval buffer (pH 6.0) at 100°C for antigenic retrieval. Endogenous peroxidase activity was blocked with 0.3% hydrogen peroxide, followed by incubation with goat serum (Gene Company Ltd.) to block non-specific binding for 2 h at room temperature. The sections were incubated with rabbit anti-human FOXC1 antibody (cat. no. HPA040670; 1:100; Sigma-Aldrich; Merck KGaA, Darmstadt, Germany) overnight at 4°C. The slides were sequentially incubated with the appropriate secondary antibody (cat. no. A0545; 1:2,000, Sigma-Aldrich; Merck KGaA) for 2 h at room temperature. Labeling was detected by adding a peroxidase-conjugated avidin-biotin complex (Dako; Agilent Technologies, Inc., Santa Clara, CA, USA) and 3,3'-diaminobenzidine (Dako; Agilent Technologies, Inc.). The immunostaining signals were counterstained with hematoxylin (Beyotime Institute of Biotechnology, Haimen, China) for 2 min. As a negative control, PBS was used in place of primary antibodies.

Staining scores were evaluated by three independent pathologists who were blind to the patients under an Olympus light microscope (BX51; Olympus Corporation, Tokyo, Japan). Expression of FOXC1 was calculated based on the proportion

of positively stained tumor cells and the intensity of staining. The proportion of tumor cells was scored as follows: 0, No positive tumor cells; 1, <10% positive; 2, 10-50% positive; 3, >50% positive. The staining extent was scored according to the area percentages as follows: 0, No staining; 1, weak staining (light yellow); 2, moderate staining (yellow brown); 3, strong staining (brown). The staining index was calculated as the staining intensity score multiplied by the proportion of positive tumor cells.

Lentiviral short hairpin (sh)RNA transduction. In order to knock down FOXC1 expression, an shRNA sequence targeting FOXC1 (Forward oligonucleotide, 5'CCGGGAGCTTTCGTC TACGACTGTACTCGAGTACAGTCGTAGACGAAAGCT CTTTTTG3'; reverse oligonucleotide, 5'AATTCAAAAAGA GCTTTCGTCTACGACTGTACTCGAGTACAGTCGTAG ACGAAAGCTC3') was designed and synthesized by Shanghai GenePharma Co., Ltd. (Shanghai, China). The sequence targeting FOXC1 was subcloned into the pLKO.1-TRC vector (Sigma-Aldrich; Merck KGaA). A scrambled non-target shRNA (shRNA; Forward oligonucleotide, 5'CCGGAATGC CTACGTTAAGCTATACCTCGAGGTATAGCTTAACGT AGGCATTTTTTTTG3'; reverse oligonucleotide, 5'AATTCA AAAAATGCCTACGTTAAGCTATACCTCGAGGTATA GCTTAACGTAGGCATT3') was used as a negative control.

To produce lentiviral particles, 8 μ g pLKO.1-shControl (scramble shRNA sequence) and pLKO.1-shFOXC1 were transfected into 293T cells (the Type Culture Collection of the Chinese Academy of Sciences, Shanghai, China) with lentiviral packaging vectors psPAX2 and pMD2.G using Lipofectamine® 2000 (Invitrogen; Thermo Fisher Scientific, Inc.), according to the manufacturer's protocol. Lentiviral particles were harvested by collecting media from 293T cells after 48 h. HeLa and SiHa cells were infected with lentiviral particles using 8 μ g/ml Polybrene (Sigma-Aldrich; Merck KGaA), and stable shRNA-expressing cell lines were selected by the addition of 2 μ g/ml puromycin (Sigma-Aldrich; Merck KGaA) to the growth medium.

Cell Counting Kit-8 (CCK-8) assays. Cell proliferation was examined using the CCK-8 assay (Dojindo Molecular Technologies, Inc., Kumamoto, Japan), according to the manufacturer's protocol. A total of 3x10³ cells were seeded into each well in 96 well plates. A total of 10 μ l CCK-8 was added into each well at 24, 48, 72 and 96 h. Following 2 h incubation, the absorbance was measured at a wavelength of 450 nm using a spectrophotometer (Tecan Infinite M200 Pro; Tecan Group, Ltd., Mannedorf, Switzerland).

Analysis of apoptosis. Cell apoptosis analysis was performed using Annexin V-fluorescein isothiocyanate (FITC) Apoptosis Detection kit I (BD Pharmingen; BD Biosciences, San Jose, CA, USA). For cell apoptosis analysis, cells (1x10⁴) were harvested with trypsin (Hyclone; GE Healthcare Life Sciences, Logan, UT, USA), centrifuged at 12,000 x g for 5 min at 4°C and incubated with 5 μ l Annexin V-FITC and 5 μ l propidium iodide for 15 min at 4°C in the dark. Following staining, cell apoptosis distribution was analyzed using a flow cytometer (Cytomics FC 500; Beckman Coulter, Inc., Brea, CA, USA) with FlowJo (version 10; Beckman Coulter, Inc.).

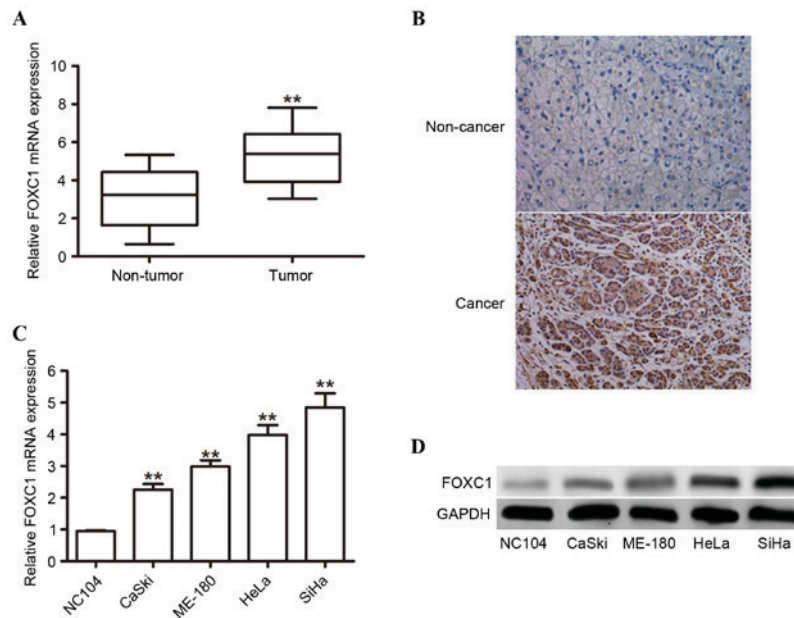


Figure 1. Upregulated FOXC1 expression in cervical cancer tissues and cell lines. (A) The relative mRNA expression levels of FOXC1 in cervical cancer tissues and control samples, detected by reverse transcription-quantitative polymerase chain reaction. (B) Representative images of immunohistochemistry analyses of FOXC1 protein expression in cervical cancer tissues and adjacent noncancerous tissues (magnification, x200). (C) The relative expression of FOXC1 in cervical cancer cell lines CaSki, HeLa, ME-180, and SiHa and the NC104 cell line. (D) Western blotting assays of the endogenous FOXC1 protein in cervical cancer cell lines and the immortalized cervical epithelial cell line. The expression levels of FOXC1 were normalized against the expression level of GAPDH. ** $P < 0.01$ vs. NC104. FOXC1, forkhead box protein C1.

Wound-healing assay. A total of 8×10^4 cells were seeded in a 6-well plate and incubated to form a confluent monolayer. Scratches were made using a 200- μ l pipette tip. Cells were washed with PBS and replaced with complete medium (10% FBS). Following incubation for 36 h, the closure of the scratch was analyzed under the microscope and images were captured using an Olympus light microscope (BX51; Olympus Corporation, Tokyo, Japan). Experiments were performed in triplicate and repeated three times.

Invasion assay. For the cell invasion assay, a filter membrane with an 8- μ m pore size (EMD Millipore, Billerica, MA, USA) was coated with Matrigel (BD Biosciences). A total of 4×10^4 cells in 100 μ l serum-free media were added to the upper chamber and the aforementioned complete medium (600 μ l) was added to the lower chamber. Following incubation for 36 h, the cells that invaded through the Matrigel membrane were fixed with 100% methanol for 30 min and stained with 0.5% crystal violet for 30 min at room temperature. A total of six random fields of each insert were counted using an Olympus light microscope at magnification x200.

Western blot analysis. Cells were lysed in ice-cold radioimmunoprecipitation assay buffer (Cell Signaling Technology, Inc., Danvers, MA, USA). Protein concentration was determined using the bicinchoninic acid assay. A total of 40 μ g protein/lane was separated by SDS-PAGE on a 10% gel and transferred to a nitrocellulose membrane (EMD Millipore). The membrane was blocked with 5% non-fat milk in 0.1% TBS-Tween-20 at room temperature for 2 h and incubated with the following primary antibodies: Rabbit anti-human FOXC1 antibody (1:1,000), rabbit anti-human phosphorylated (p)-RAC- α serine/threonine-protein kinase (AKT) antibody

(Ser473; cat. no. 9271; 1:1,000; Cell Signaling Technology, Inc.), rabbit anti-human AKT antibody (cat. no. 9272; 1:1,000; Cell Signaling Technology, Inc.), rabbit anti-human proto-oncogene c-Myc (c-Myc) antibody (cat. no. 9402; 1:1,000; Cell Signaling Technology, Inc.), rabbit anti-human apoptosis regulator B cell lymphoma-2 (Bcl-2) antibody (cat. no. 2872; 1:1,000; Cell Signaling Technology, Inc.) or rabbit anti-human GAPDH antibody (cat. no. 2118; 1:1,000; Cell Signaling Technology, Inc.) at 4°C overnight. The specific binding on the membrane was probed with horseradish peroxidase-conjugated anti-rabbit secondary antibody (cat. no. 7071; 1:1,000; Cell Signaling Technology, Inc.) for 2 h at room temperature. Bands were visualized using a nitrotyrosine enzyme linked immunosorbent assay kit (cat. no. 17-376; Merck KGaA).

Statistical analysis. The paired sample t-test was used to make comparisons between two groups and one-way analysis of variance followed by Tukey's post-hoc test were performed to assess the difference between >2 groups. The χ^2 test was utilized to evaluate the association between FOXC1 mRNA expression and clinicopathological characteristics. The Kaplan-Meier estimator and log-rank test were used to evaluate the OS of cervical cancer patients. Data are presented as the mean \pm standard deviation of three experimental repeats and all statistical analyses were performed using GraphPad Prism (version 5.01; GraphPad Software, Inc., La Jolla, CA, USA). $P < 0.05$ was considered to indicate a significant difference.

Results

FOXC1 expression is upregulated in human cervical cancer tissues and cell lines. To investigate the role of FOXC1 in human cervical cancer tissues, the expression levels between

Table I. Association between FOXC1 expression and clinicopathological parameters of cervical cancer.

Clinicopathological parameters	Total (n=76)	FOXC1 expression		P-value
		High (n=38)	Low (n=38)	
Age, years				0.2055
≤45	22	8	14	
>45	54	30	24	
FIGO stage				0.0093
I	48	19	29	
II	28	20	8	
Differentiation grade				0.3506
Well/Moderate	45	20	25	
Poor	31	18	13	
Tumor size (cm)				0.2264
≤4	50	22	28	
>4	26	16	10	
Lymph node metastasis				0.0178
Yes	20	15	5	
No	56	23	33	
Vascular involvement				0.1332
Yes	23	15	8	
No	53	23	30	
Stromal invasion				0.3801
<66%	61	26	25	
≥66%	15	10	5	
Vaginal involvement				0.7361
Yes	10	6	4	
No	66	32	34	
Parametrial infiltration				0.6745
Yes	6	4	2	
No	70	34	36	

FIGO, International Federation of Gynecology and Obstetrics; FOXC1, forkhead box protein C1.

76 cervical cancer tissues and 34 non-malignant control samples were compared using RT-qPCR. The mRNA expression level of FOXC1 was observed to be significantly increased in cancerous tissues compared with control samples (Fig. 1A). IHC staining detected FOXC1 protein in 76.3% (58/76) of paraffin-embedded cervical cancer tissues, whereas a lower staining index was calculated in adjacent non-cancerous tissues (Fig. 1B). The mRNA expression levels of FOXC1 in four cervical cancer cell lines (CaSki, HeLa, ME-180 and SiHa) and the non-malignant cell line NC104 were evaluated using RT-qPCR. The results demonstrated that the expression levels of FOXC1 in all four cell lines were significantly upregulated compared with NC104 cells (Fig. 1C). In addition, western blotting was performed to confirm that the protein expression level of FOXC1 was increased in cervical cancer cell lines (Fig. 1D). These results suggested that FOXC1 may serve important roles in human cervical cancer.

Association between expression of FOXC1 and clinical characteristics in cervical cancer. To determine the

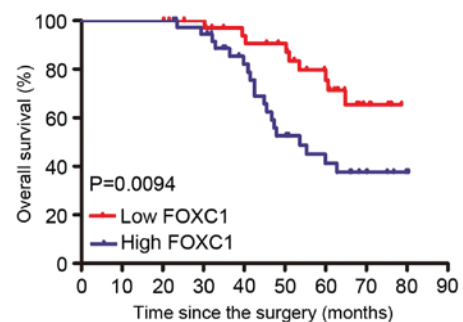


Figure 2. Kaplan-Meier survival curves. Kaplan-Meier curves for survival time in patients with cervical cancer, divided according to FOXC1 expression, with significantly shorter survival times for patients with high FOXC1 expression compared with those with low FOXC1 expression. FOXC1, forkhead box protein C1.

clinical relevance of FOXC1 in cervical cancer, the present study examined the association between FOXC1 mRNA

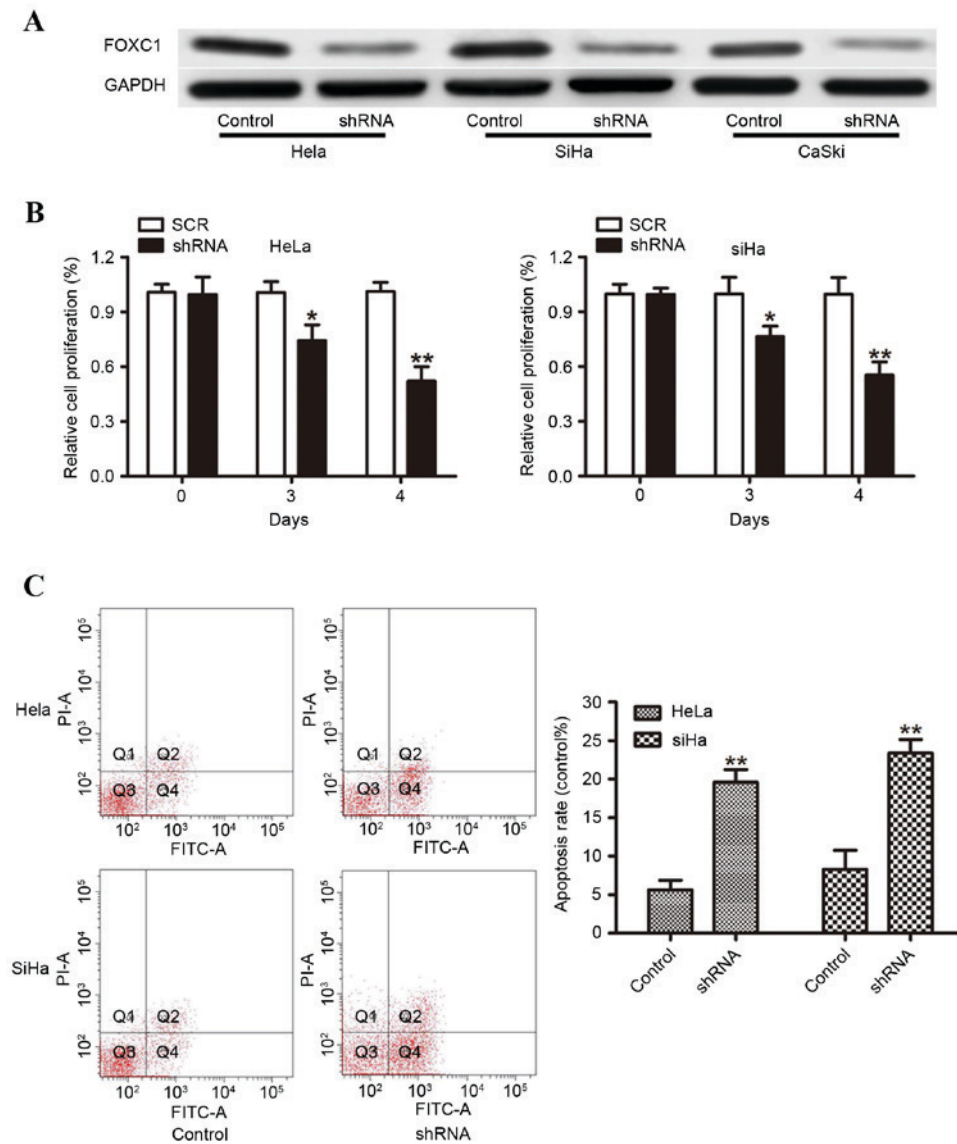


Figure 3. FOXC1 silencing inhibits cervical cancer cell growth *in vitro*. (A) Western blotting was performed to confirm the effective knockdown of FOXC1. (B) Effect of FOXC1 on HeLa and SiHa cell proliferation was measured by Cell Counting Kit-8 assay. (C) Apoptosis was detected by Annexin V-FITC and PI double staining and analyzed by flow cytometry when FOXC1 was silenced. * $P < 0.05$, ** $P < 0.01$ vs. shRNA control. FOXC1, forkhead box protein C1; FITC, fluorescein isothiocyanate; PI, propidium iodide; shRNA, short hairpin RNA.

expression and various clinicopathological factors (Table I). The median expression level of FOXC1 was used as a cut-off point to divide all patients into two groups: Patients who expressed FOXC1 at levels above the cut-off value were assigned to the high expression group ($n=38$), and those with expression less than the cut-off value were assigned to the low expression group ($n=38$). A high FOXC1 expression level was demonstrated to be significantly associated with lymph node metastasis ($P=0.0178$) and FIGO stage ($P=0.0093$). However, a high FOXC1 expression level was not associated with other clinicopathological factors, including age, vaginal involvement, tumor histology, and tumor size. Furthermore, the Kaplan Meier analysis revealed that patients with a high FOXC1 expression have a poorer survival compared with those exhibiting a decreased expression of FOXC1 (Fig. 2). The results revealed that FOXC1 expression served as a potential independent prognostic factor in patients with cervical cancer.

Knockdown of FOXC1 inhibits cervical cancer cell proliferation and induces apoptosis. As FOXC1 was demonstrated to be increased in cervical cancer tissues, the present study then knocked down FOXC1 using shRNA to investigate the biological function of FOXC1 *in vitro*. HeLa, SiHa and CaSki cells with high endogenous FOXC1 expression were selected for the knockdown. Western blot analysis was performed to detect the knockdown efficiencies, and the protein expression of FOXC1 was significantly decreased in FOXC1 shRNA-transduced cells compared with control shRNA-transduced cells (Fig. 3A). Cellular proliferation was assessed using a CCK-8 assay and the results demonstrated that FOXC1 silencing resulted in a significant inhibition of HeLa and SiHa cell proliferation at 72 and 96 h (Fig. 3B). To further investigate the effect of FOXC1 on cell survival, the present study measured cell apoptosis using flow cytometry. As presented in Fig. 3C, knockdown of FOXC1 led to a significant increase in apoptosis (Fig. 3C). These data

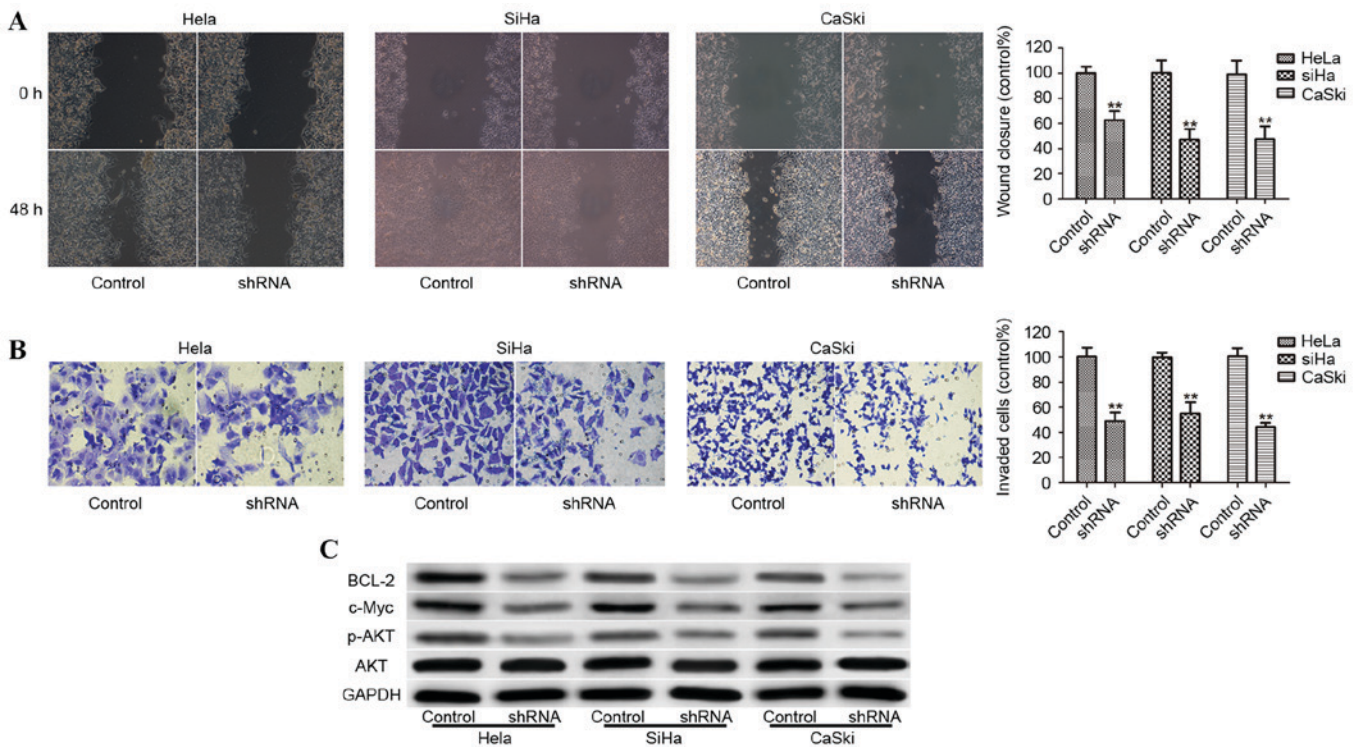


Figure 4. Knockdown of FOXC1 decreases migratory and invasive abilities of cervical cancer cells. (A) Wound-healing capacity of Hela, SiHa and CaSki cells transfected with control shRNA or FOXC1 shRNA. (B) Matrigel-coated Transwell cell invasion assays of control cells and FOXC1 shRNA stably transfected cervical cancer cells. (C) p-AKT, c-Myc, and Bcl-2 protein levels were downregulated by FOXC1 shRNA in Hela, SiHa and CaSki cells. ** $P < 0.01$ vs. shRNA control. shRNA, short hairpin RNA; FOXC1, forkhead box protein C1; p, phosphorylated; AKT, RAC- α serine/threonine-protein kinase (AKT); c-Myc, proto-oncogene c-Myc; Bcl-2, apoptosis regulator B cell lymphoma-2.

suggested that FOXC1 exhibited a key role in cervical cancer cell survival.

FOXC1 silencing attenuates cell invasion. To further evaluate the effect of FOXC1 on cervical cancer progression, the present study detected the influence on cervical cancer cell migration and invasion. Migration was assessed via a wound-healing assay, whereas invasion was assessed using a Matrigel invasion assay. FOXC1 silencing significantly delayed wound healing of Hela, SiHa and CaSki compared with control-transduced cells (Fig. 4A). Furthermore, FOXC1 knockdown in Hela, SiHa and CaSki cells significantly decreased the invasion of cells through the Matrigel basement membrane (Fig. 4B). To study the mechanism implicated in the reduction of growth rate and invasion in cervical cancer cell, the relative levels of proteins that are direct or indirect targets of FOXC1 were analyzed. As presented in Fig. 4C, the expression of p-AKT, c-Myc and Bcl-2 protein in FOXC1 shRNA-transduced cells was decreased compared with control shRNA-transduced cells (Fig. 4C).

Discussion

Several reports have demonstrated that aberrant FOXC1 expression is associated with the development and progression of a variety of cancers, including breast, hepatocellular carcinoma, pancreatic and non-small cell lung cancers (9,12,14,15). However, FOXC1 expression and its potential role in cervical cancer remains unclear. The present study aimed to explore the expression of FOXC1 in cervical cancers compared with

benign cervical tissues, assess its association with clinicopathological parameters, and investigate its prognostic value for cervical cancer patients.

The present study demonstrated that the mRNA level of FOXC1 in cervical cancer tissues was significantly increased compared with non-cancerous cervical tissues. Consistent with previous studies, an increased FOXC1 expression was revealed to be positively associated with lymph node metastasis, FIGO stage, and poor prognosis (9,13,15). It has previously been demonstrated that FOXC1 is overexpressed in human cancer and acts as an oncogene to promote proliferation and metastasis. A previous study suggests that non-canonical Hedgehog signaling is mediated by FOXC1 to determine the basal-like breast cancer stem-like phenotype and anti-Hedgehog sensitivity (19). FoxC1 has additionally been demonstrated to act as a transcriptional factor involved in tumor cell growth via regulating the cell cycle (12,20,21). In accordance with the results of previous studies, the present study demonstrated that FOXC1 silencing decreased cell proliferation and induced cell apoptosis. The involvement of FOXC1 in regulating tumor metastasis has been previously described in breast cancer, hepatocellular carcinoma, melanoma, nasopharyngeal carcinoma, and non-small cell lung cancer (8,9,17,19,22). The present study demonstrated that shRNA-mediated FOXC1 downregulation yielded a significant decrease in cell migration and invasion. The phosphoinositide 3-kinase (PI3K)-Akt signaling pathway has been previously demonstrated to be important in cancer cell proliferation and invasion (23-25). Depletion of FOXC1 in cervical cancer cells significantly reduced expression levels of p-AKT, c-Myc and Bcl-2, which

are known to exhibit important roles in tumor progression. The data suggested that activation of PI3K/AKT signaling pathways were involved in FOXC1-mediated cell proliferation, migration, and invasion of cervical cancer cells.

In conclusion, the results of the present study demonstrated that FOXC1 was highly expressed in cervical cancer and increased FOXC1 expression was positively associated with metastasis, FIGO stage, and OS. Functional studies suggested that knockdown of FOXC1 suppressed cell proliferation, migration and invasion by regulating the AKT signaling pathway. The results suggested that FOXC1 exhibits an important role in cervical cancer and may act as a potential therapeutic target for future treatment of the disease.

Acknowledgements

The present study was supported by the Natural Science Foundation of Heilongjiang Province, China (grant no. H201385).

References

- Siegel R, Ma J, Zou Z and Jemal A: Cancer statistics, 2014. *CA Cancer J Clin* 64: 9-29, 2014.
- Denny L, de Sanjose S, Mutebi M, Anderson BO, Kim J, Jeronimo J, Herrero R, Yeates K, Ginsburg O and Sankaranarayanan R: Interventions to close the divide for women with breast and cervical cancer between low-income and middle-income countries and high-income countries. *Lancet* 389: 861-870, 2017.
- Waggoner SE: Cervical cancer. *Lancet* 361: 2217-2225, 2003.
- Molano M, Moreno-Acosta P, Morales N, Burgos M, Buitrago L, Gamboa O, Alvarez R, Garland SM, Tabrizi SN, Steenbergen RD and Mejía JC: Association between type-specific HPV infections and hTERT DNA methylation in patients with invasive cervical cancer. *Cancer Genomics Proteomics* 13: 483-491, 2016.
- Schiffman M and Solomon D: Clinical practice. Cervical-cancer screening with human papillomavirus and cytologic cotesting. *N Engl J Med* 369: 2324-2331, 2013.
- Muñoz N, Franceschi S, Bosetti C, Moreno V, Herrero R, Smith JS, Shah KV, Meijer CJ and Bosch FX; International Agency for Research on Cancer. Multicentric Cervical Cancer Study Group: Role of parity and human papillomavirus in cervical cancer: The IARC multicentric case-control study. *Lancet* 359: 1093-1101, 2002.
- Rauh-Hain JA, Clemmer JT, Bradford LS, Clark RM, Growdon WB, Goodman A, Boruta DM II, Schorge JO and del Carmen MG: Racial disparities in cervical cancer survival over time. *Cancer* 119: 3644-3652, 2013.
- Sizemore ST and Keri RA: The forkhead box transcription factor FOXC1 promotes breast cancer invasion by inducing matrix metalloprotease 7 (MMP7) expression. *J Biol Chem* 287: 24631-24640, 2012.
- Xia L, Huang W, Tian D, Zhu H, Qi X, Chen Z, Zhang Y, Hu H, Fan D, Nie Y and Wu K: Overexpression of forkhead box C1 promotes tumor metastasis and indicates poor prognosis in hepatocellular carcinoma. *Hepatology* 57: 610-624, 2013.
- Sun J, Ishii M, Ting MC and Maxson R: Foxc1 controls the growth of the murine frontal bone rudiment by direct regulation of a Bmp response threshold of Msx2. *Development* 140: 1034-1044, 2013.
- Jin Y, Han B, Chen J, Wiedemeyer R, Orsulic S, Bose S, Zhang X, Karlan BY, Giuliano AE, Cui Y and Cui X: FOXC1 is a critical mediator of EGFR function in human basal-like breast cancer. *Ann Surg Oncol* 21 (Suppl 4): S758-S766, 2014.
- Xu ZY, Ding SM, Zhou L, Xie HY, Chen KJ, Zhang W, Xing CY, Guo HJ and Zheng SS: FOXC1 contributes to microvascular invasion in primary hepatocellular carcinoma via regulating epithelial-mesenchymal transition. *Int J Biol Sci* 8: 1130-1141, 2012.
- Wei LX, Zhou RS, Xu HF, Wang JY and Yuan MH: High expression of FOXC1 is associated with poor clinical outcome in non-small cell lung cancer patients. *Tumour Biol* 34: 941-946, 2013.
- Song Y, Washington MK and Crawford HC: Loss of FOXA1/2 is essential for the epithelial-to-mesenchymal transition in pancreatic cancer. *Cancer Res* 70: 2115-2125, 2010.
- Ray PS, Wang J, Qu Y, Sim MS, Shamonki J, Bagaria SP, Ye X, Liu B, Elashoff D, Hoon DS, *et al*: FOXC1 is a potential prognostic biomarker with functional significance in basal-like breast cancer. *Cancer Res* 70: 3870-3876, 2010.
- Saslow D, Solomon D, Lawson HW, Killackey M, Kulasingam SL, Cain J, Garcia FA, Moriarty AT, Waxman AG, Wilbur DC, *et al*: American Cancer Society, American Society for Colposcopy and Cervical Pathology, and American Society for Clinical Pathology screening guidelines for the prevention and early detection of cervical cancer. *Am J Clin Pathol* 137: 516-542, 2012.
- Wu T, Chen X, Peng R, Liu H, Yin P, Peng H, Zhou Y, Sun Y, Wen L, Yi H, *et al*: Let7a suppresses cell proliferation via the TGF- β /SMAD signaling pathway in cervical cancer. *Oncol Rep* 36: 3275-3282, 2016.
- Livak KJ and Schmittgen TD: Analysis of relative gene expression data using real-time quantitative PCR and the 2(-Delta Delta C(T)) method. *Methods* 25: 402-408, 2001.
- Ou-Yang L, Xiao SJ, Liu P, Yi SJ, Zhang XL, Ou-Yang S, Tan SK and Lei X: Forkhead box C1 induces epithelial-mesenchymal transition and is a potential therapeutic target in nasopharyngeal carcinoma. *Mol Med Rep* 12: 8003-8009, 2015.
- Han B, Qu Y, Jin Y, Yu Y, Deng N, Wawrowsky K, Zhang X, Li N, Bose S, Wang Q, *et al*: FOXC1 activates smoothed-independent hedgehog signaling in basal-like breast cancer. *Cell Rep* 13: 1046-1058, 2015.
- Chen S, Jiao S, Jia Y and Li Y: Effects of targeted silencing of FOXC1 gene on proliferation and in vitro migration of human non-small-cell lung carcinoma cells. *Am J Transl Res* 8: 3309-3318, 2016.
- Wang J, Ray PS, Sim MS, Zhou XZ, Lu KP, Lee AV, Lin X, Bagaria SP, Giuliano AE and Cui X: FOXC1 regulates the functions of human basal-like breast cancer cells by activating NF- κ B signaling. *Oncogene* 31: 4798-4802, 2012.
- Wang J, Li L, Liu S, Zhao Y, Wang L and Du G: FOXC1 promotes melanoma by activating MST1R/PI3K/AKT. *Oncotarget* 7: 84375-84387, 2016.
- Wang Z, Qu L, Deng B, Sun X, Wu S, Liao J, Fan J and Peng Z: STYK1 promotes epithelial-mesenchymal transition and tumor metastasis in human hepatocellular carcinoma through MEK/ERK and PI3K/AKT signaling. *Sci Rep* 6: 33205, 2016.
- Yang J, Qin G, Luo M, Chen J, Zhang Q, Li L, Pan L and Qin S: Reciprocal positive regulation between Cx26 and PI3K/Akt pathway confers acquired gefitinib resistance in NSCLC cells via GJIC-independent induction of EMT. *Cell Death Dis* 6: e1829, 2015.



This work is licensed under a Creative Commons Attribution 4.0 International (CC BY 4.0) License.